Morphological Behavior of Lipid Bilayers Induced by Melittin near the Phase Transition Temperature

Shuichi Toraya,* Takashi Nagao,† Kazushi Norisada,† Satoru Tuzi,† Hazime Saitô,†‡ Shunsuke Izumi,‡§ and Akira Naito*

*Graduate School of Engineering, Yokohama National University, Yokohama 240-8501, Japan; †Department of Life Science, Graduate School of Science, Himeji Institute of Technology, Harima Science Garden City, Kamigori, Hyogo 678-1297, Japan; and ‡Center for Quantum Life Sciences and §Graduate School of Science, Hiroshima University, Higashi-Hiroshima, 739-8526, Japan

ABSTRACT Morphological changes of DMPC, DLPC, and DPPC bilayers containing melittin (lecithin/melittin molar ratio of 10:1) around the gel-to-liquid crystalline phase transition temperatures (*T*c) were examined by a variety of biophysical methods. First, giant vesicles with the diameters of ~20 μm were observed by optical microscopy for melittin-DMPC bilayers at 27.9°C. When the temperature was lowered to 24.9°C (*T*c = 23°C for the neat DMPC bilayers), the surface of vesicles became blurred and dynamic pore formation was visible in the microscopic picture taken at different exposure times. Phase separation and association of melittin molecules in the bilayers were further detected by fluorescent microscopy and mass spectrometry, respectively. These vesicles disappeared completely at 22.9°C. It was thus found that the melittin-lecithin bilayers reversibly undergo their fusion and disruption near the respective *T*cs. The fluctuation of lipids is, therefore, responsible for the membrane fusion above the *T*c, and the association of melittin molecules causes membrane fragmentation below the *T*c. Subsequent magnetic alignments were observed by solid-state ^{31}P NMR spectra for the melittin-lecithin vesicles at a temperature above the respective *T*cs. On the other hand, additional large amplitude motion induced by melittin at a temperature near the *T*c breaks down the magnetic alignment.

INTRODUCTION

Melittin is a hexacosapeptide with a primary structure of Gly Ile-Gly-Ala-Val-Leu-Lys-Val-Leu-Thr-Thr-Gly-Leu-Pro-Ala-Leu-Ile-Ser-Trp-Ile-Lys-Arg-Lys-Arg-Gln-Gln-NH_2 and is a main component of a honeybee venom, *Apis mellifera* (1). Melittin has a powerful hemolytic activity (2) in addition to voltage-dependent ion conductance across planar lipid bilayer (3,4) and selective micellization of bilayers as well as membrane fusion (5–8). At a moderately high concentration, melittin is known to cause the breakdown of lipid bilayers into micelles in a similar manner to solubilization by detergent below the gel-to-liquid crystalline phase transition temperature (*T*c) and vesiculation from micelles above the *T*c (6). The phenomenon has been extensively studied by means of light scattering, freeze-fracture electron microscopy, and nuclear magnetic resonance spectroscopy to understand the action of melittin on lipid bilayers (6,7,9–11). As the temperature is lowered to the gel phase, the lipid bilayers break down into small particles. Upon raising the temperature back above the *T*c, the small particles reform to unilamellar vesicles. This phase-dependent lysis and fusion are readily observable by ^{31}P and ^{2}H NMR spectroscopy (7,11). Dufourc et al. proposed that the bilayer discs surrounded by a belt of melittin molecules are formed at a temperature below the *T*c (9). The presence of negatively charged lipids reduced the proportion of lysed vesicles (12), although melittin binds strongly with negatively charged lipids by the electrostatic effect (13).

Melittin takes a disordered conformation (14,15) and α-helical structure (16) in dilute aqueous and methanol solutions as a monomer, respectively. In contrast, melittin forms tetramer with an α-helical structure in high ionic strength and pH in an aqueous solution (17). In crystalline states, a single polypeptide chain of melittin consists of two α-helical rods, residues 1–10 and 13–26, making a kink angle of ~120° and forming a tetrameric complex as revealed by x-ray diffraction studies of a 2 Å resolution (18,19). In membrane environments, melittin forms an α-helical structure when it binds to dodecylphosphocholine micelles with the α-helical axis parallel to the micelle-water interface (20). Transferred nuclear Overhauser enhancement analysis indicated divergent conformations for the region Arg^{22}-Gln^{26} of melittin bound to lipid bilayers (21).

The orientations of melittin in the lipid bilayers depend on the conditions such as peptide/lipid ratio and degree of hydration. At the low peptide/lipid ratio, the helical segments are oriented parallel to the bilayer planes as studied by polarized attenuated total internal reflection-Fourier transform infrared spectroscopy (PATIR-FTIR) in supported membranes (22), accessibility measurements of spin-labeled melittin by chromium oxalate (23), ^{13}C NMR in the presence of an aqueous shift reagent (24), and measurement of hydrogen-deuterium exchange rate (25), which indicate that the melittin lies on the membrane surface. An x-ray absolute-scale refinement study for melittin of 1 mol % concentration in the lipid deposited on curved substrates revealed that the helical axis is aligned parallel to the bilayer plane at the depth of the glycerol groups (26). At a peptide/lipid ratio >4 mol

Submitted January 10, 2005, and accepted for publication August 8, 2005.

Address reprint requests to Akira Naito, Fax: 81-45-339-4251; E-mail: naito@ynu.ac.jp.

0006-3495/05/11/3214/09 $2.00

doi: 10.1529/biophysj.105.059311

% in the lipid bilayers, melittin reorients into a transmembrane (26). The structure of melittin bound to a mechanically oriented ditetradecylphosphatidylcholine (DTPC) membrane has been examined to take a transmembrane α-helix (27). It was revealed that the melittin (9 mol %) in the 86% hydrated lipid bilayer vesicles consisting of dimyristoylphosphatidylcholine (DMPC), dilauroylphosphatidylcholine (DLPC), and dipalmitoylphosphatidylcholine (DPPC) takes a pseudotransmembrane α-helical structure (28,29). The membrane-bound melittin further turned out to be rotating rapidly about the axis parallel to the bilayer normal as a result of lateral diffusion. The interhelical angles of a transmembrane helix of melittin in the hydrated vesicles were determined to be $\sim$120° for DLPC and DPPC bilayers. This angle increases to 140° in the hydrated gel state of DTPC multilayers (30). This difference can be attributed to the different lipid conditions. As to the degree of hydration, an attenuated total reflection infrared study showed that the α-helix of melittin is oriented parallel and perpendicular to the bilayer surface in hydrated single planar and dry phospholipids multilayers, respectively (31). Further study will be required because the orientations of peptides in the lipid bilayers are very important for understanding the action of melittin on the membrane.

One of the interesting properties of lipid bilayers containing melittn is an ability of highly magnetic ordering in the presence of a strong magnetic field (28,29,32) in contrast to the partially magnetic ordering in pure and mixed phospholipid bilayer systems (33–37). Actually, the long axis of the elongated vesicle is aligned parallel to the applied magnetic field as magnetically oriented vesicle systems (MOVS) arising from the total diamagnetic susceptibility of phospholipids in the whole vesicles. Therefore, MOVS can be conveniently used to determine the structure and orientation of melittin bound to the membrane (28,29). This is because the melittin bound to the membrane is simultaneously aligned to the applied magnetic field.

In this study, we demonstrate a more detailed morphological behavior of melittin-lecithin bilayers around the phase transition temperature as revealed by optical microscopy, solid-state ^{31}P NMR, ion selective electrode and matrix-assisted laser desorption ionization-time of flight-mass spectrometry (MALDI-TOF MS) to gain insight into the molecular mechanism of lytic and fusion activity of melittin on a variety of lecithin membranes. We found that melittin induced formations of giant vesicles from DLPC, DMPC, and DPPC bilayers with diameters of $\sim$20 μm, which permits one to examine their morphological behavior in real time by optical microscope and solid-state ^{31}P NMR observations.

MATERIALS AND METHODS

Sample preparation

Melittin was synthesized by a solid phase method with an Applied Biosystems (Foster City, CA) 431A peptide synthesizer. Synthesized peptides were purified using a Waters (Milford, MA) 600E high-performance liquid chromatography system with a BONDASHERE C18 reversed phase column (Waters); >95% purity was estimated from the chromatogram. A total of 50 mg of melittin and lecithin molecules (DLPC, DMPC, and DPPC) with a melittin/lecithin molar ratio of 1:10 were dissolved in chloroform, and the solvent was subsequently evaporated in vacuo followed by hydration with 900 μl of Tris buffer (20 mM Tris, 100 mM NaCl, and pH 7.5). A freeze-and-thaw cycle was repeated 10 times, followed by centrifugation to concentrate the bilayers at 28°C. This process was repeated three times, and finally the total volume was adjusted to 300 μl containing 50 mg of lecithin and melittin. The lipid bilayers were placed in a glass sample tube and sealed with glue to prevent dehydration during NMR measurements.

Cross-linking experiments

The melittin-DMPC bilayers were incubated at 15°C, 25°C, and 35°C with a cross-linking reagent, bis(sulfosuccinimidyl)adipate (BS^2) (400-fold molar excess) in 15 mM sodium phosphate buffer, pH 7.5, containing 20 mM NaCl. BS^2 was allowed to react with the amino groups of Lys residues in melittin and subsequently allowed to link the melittin molecules within their distances of 7 Å. After 60 min, the reactions were quenched by adding 5 μL of 100 mM ammonium bicarbonate. The products were analyzed by MALDI-TOF MS spectrometry.

Solid-state NMR measurements

Static ^{31}P NMR spectra using the 90° excitation pulse of 5 μs and the recycle time of 2 s were recorded on a Chemagnetics (Fort Collins, CO) CMX-400 Infinity NMR spectrometer at 161.98 MHz under high power proton decoupling with the radio frequency pulse of 50 kHz. ^{31}P chemical shifts values were referred to 85% H_3PO_4. NMR spectra were acquired after waiting 30 min at various temperatures to equilibrate the temperatures of the lipid bilayers when the temperature was changed.

Optical microscopic measurements

Microscopic pictures were obtained using a Carl Zeiss (Jena, Germany) Axiophot microscope equipped with differential interference optics. Fluorescent microscopic pictures were recorded on an Olympus BX50-type equipped with a wideband-U excitation unit. Temperatures of bilayer dispersions adjusted as described above were controlled in a temperature range from 5° to 40°C using a temperature-controlled stage for the microscope (TOKAI HIT, Shizuoka, Japan). A nitrogen gas stream was used for a low temperature experiment to prevent vapor condensation. The temperature of the sample was subsequently corrected by a Peltier-mode cooling-heating apparatus (Japan High Tech, Fukuoka, Japan) and a probe-clip press-seal incubation chamber. The lipid bilayer samples used for the NMR measurements were diluted five times with Tris buffer, and 30 μl of the samples were placed on a glass plate and covered by a thin cover glass. The edge part of the cover glass was sealed with a clear nail polish to prevent dehydration.

Measurements of potassium ion leaking

Potassium ion-selective and reference electrodes (Horiba, Kyoto, Japan) were used to measure the leakage of potassium ions from the vesicle by adding Triton X-100 as a detergent. Lipid bilayer dispersions (0.4 ml) were prepared with buffer (20 mM Tris, 100 mM KCl, and pH 7.4) followed by adding 100 ml of Tris buffer containing 100 mM NaCl, and subsequently 1 ml of 5% w/v Triton X-100 aqueous solution was added to the solution in drops to dissolve the lipid bilayers while keeping temperatures at 40°C and 2°C.

Measurements of MALDI-TOF MS spectra

MALDI-TOF MS spectra were recorded on an ultraflex TOF instrument (Bruker Daltonics, Bremen, Germany) equipped with a nitrogen laser operated at 337 nm. All MALDI-TOF results were obtained in the linear positive mode using α-cyano-4-hydroxycinnamic acid (saturated solution in 50% acetonitrile with 0.1% trifluoroacetic acid) as a matrix. Analytes were prepared by mixing 0.5 μL of the products of cross-linking experiments with 0.5 μL of the matrix solution on a MALDI plate and allowed to dry at room temperature in a hood before inserting into the spectrometer. Mass spectra were calibrated with angiotensin II (1046.54 Da), angiotensin I (1296.68 Da), substance P (1347.74 Da), bombesin (1619.82 Da), adrenocorticotropic hormone (ACTH18-39) (2465.20 Da), and insulin (5733.54 Da). All mass data are reported as average values.

RESULTS

Microscopic observation of morphological changes in melittin-DMPC bilayer systems

Fig. 1 shows the microscopic pictures of melittin-DMPC bilayers taken with the exposure time of 0.70 s. Giant vesicles with diameters >20 μm were observed after the melittin-DMPC dispersion was incubated at 27.9°C for 3 h (Fig. 1 *A*). Vesicle fusion was clearly seen at the center region of Fig. 1 *A*. When the temperature was lowered to 24.9°C, blurred surfaces of vesicles were seen (Fig. 1 *B*). This temperature is ~2°C higher than the *T*c of the neat DMPC (*T*c = 23°C). When the temperature was further lowered to 22.9°C, the vesicles disappeared completely (Fig. 1 *C*). When the temperature was raised back to 27.9°C (Fig. 2 *A*), small spherical vesicles with the diameters of ~5 μm appeared after 30 min (Fig. 2 *B*) and fused into larger vesicles with the diameters of ~20 μm after 2 h taken with the exposure time of 0.70 s (Fig. 2 *C*). Therefore, it is obvious that lysis and fusion occurred reversibly near the *T*c.

Since the presence of blurred contours of the vesicles seems to be due to a dynamic change of their surface states, the exposure time in taking the snapshots was shortened to gain insight into an instantaneous image of the dynamical change. Fig. 3 shows microscopic pictures of the melittin-DMPC bilayer systems in a lytic process taken with the exposure time of 0.05 s. It is noteworthy that a number of

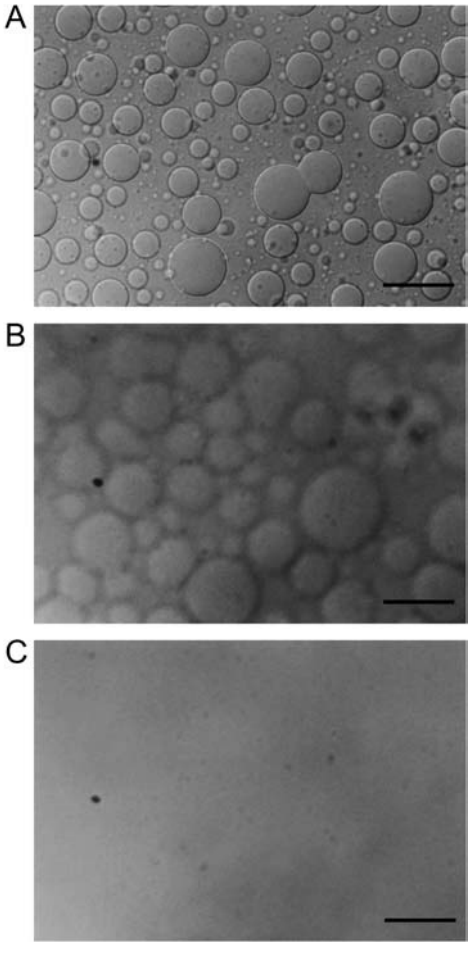

FIGURE 1 Microscopic pictures of the melittin-DMPC bilayer systems in a lytic process taken at 27.9°C (*A*), 24.9°C (*B*), and 22.9°C (*C*) with the exposure time of 0.70 s. The scale bar represents 50 μm.

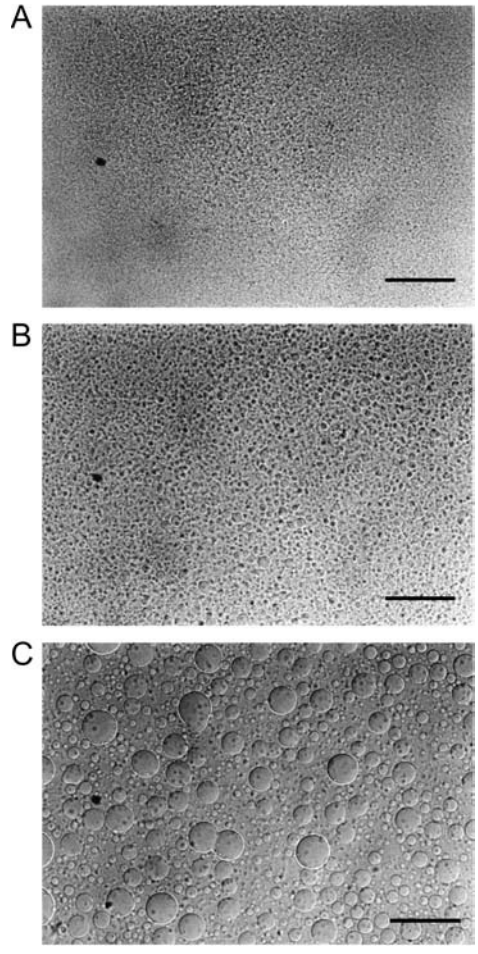

FIGURE 2 Microscopic pictures of the melittin-DMPC bilayer systems at the time of a fusion process of 5 min (*A*), 30 min (*B*), and 120 min (*C*) after the temperature was raised to 27.9°C taken with the exposure time of 0.70 s. The scale bar represents 50 μm.

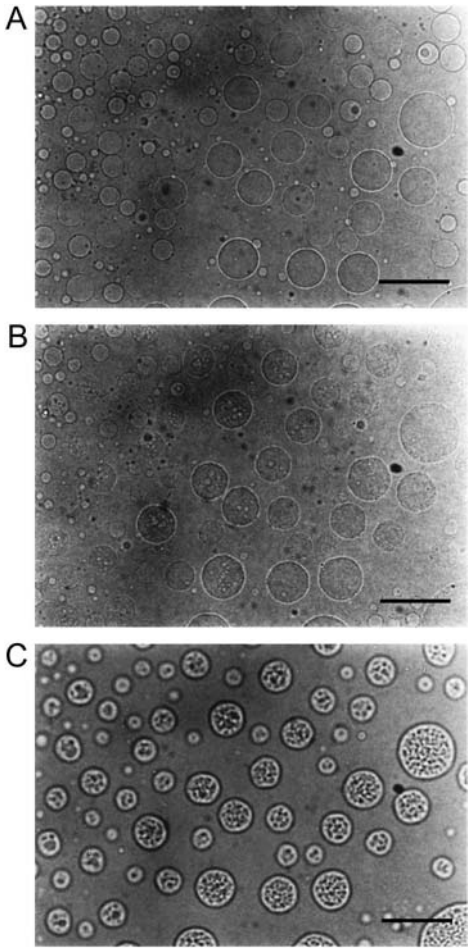

FIGURE 3 Microscopic pictures of the melittin-DMPC bilayer systems in a lytic process taken at 27.9°C (*A*), 24.9°C (*B*), and 25.9°C (*C*) with the exposure time of 0.05 s. The scale bar represents 50 μm.

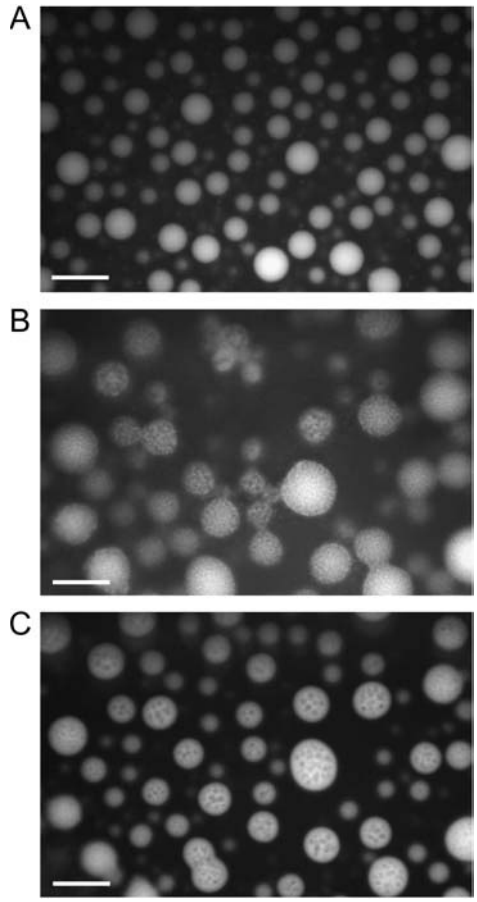

FIGURE 4 Fluorescent microscopic pictures of the melittin-DMPC bilayer systems at 27.9°C (*A*), 24.9°C (*B*), and 25.9°C (*C*). Fluorescence of Trp residue was observed. The scale bar represents 50 μm.

pores were visible on the surface of the vesicles after the temperature was lowered from 27.9° (Fig. 3 *A*) to 24.9°C (Fig. 3 *B*). Static pored vesicles were further observed as the rate of opening, and closing pores was decreased by raising the temperature to 25.9°C (Fig. 3 *C*).

Fig. 4 shows the fluorescent microscopic picture of the melittin-DMPC systems arising from Trp residue as an intrinsic fluorescent probe. It is noticed that only vesicles are illuminating at 27.9°C from melittin strongly bound to the DMPC bilayers and homogeneously distributed in the vesicles at a temperature above the *T*c (Fig. 4 *A*). It appears that the bilayers form multilamellar vesicles because the center part of the vesicle illuminates more strongly than the edge part does. In contrast, melittin seems to be distributed rather heterogeneously in the vesicle at 24.9°C that is near the *T*c (Fig. 4 *B*)—the illuminated areas diffused to the solution area—because the formed small particles were dissolved into the solution. Nevertheless, the pores were stable and melittin distributed back to the membranes in the vesicles when the temperature is raised up to 25.9°C (Fig. 4 *C*). These results indicate that melittin is distributed homogeneously in the membrane at a temperature above the *T*c, whereas heterogeneously distributing or phase separation occurs near the *T*c. Such heterogeneous distribution might be related to the formation of pores, and consequently the fragmentation can be completed at a temperature below the *T*c.

Magnetic alignment of DMPC bilayers containing melittin revealed by ^{31}P NMR

Fig. 5 shows the ^{31}P NMR spectra of the melittin-DMPC bilayers hydrated with Tris buffer recorded at various temperatures. Immediately after the sample was placed in the magnetic field, the ^{31}P NMR spectrum of an axially symmetric powder pattern characteristic of the liquid crystalline phase was initially recorded at 40°C (Fig. 5, *left top trace*). The chemical shift values for the perpendicular ($\delta_{\perp}$) and parallel ($\delta_{//}$) components are summarized in Table 1. It is noticed, however, that the upper field edge (perpendicular component) is more intense than the lower field edge (parallel component) as compared with a normally axially

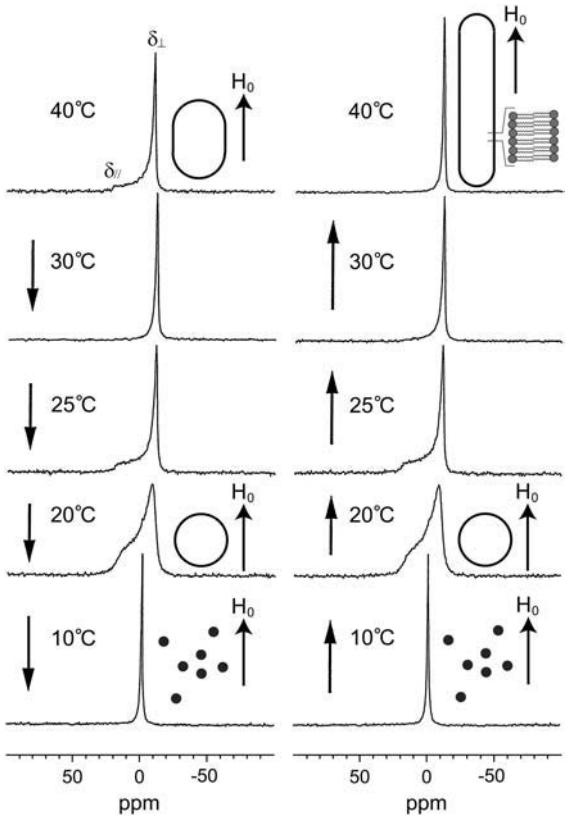

FIGURE 5 Temperature variation of the ^{31}P NMR spectra of the melittin-DMPC bilayer systems. The arrows indicate the direction of the temperature variation. H_0 indicates the direction of the static magnetic field. The shapes of the vesicles are also depicted.

symmetric powder pattern. This finding indicates that the DMPC bilayer planes are partially aligned to the applied magnetic field by forming elongated vesicles (Fig. 5). When the temperature was lowered to 30°C, the intensity of the upper field edge of the powder pattern was further increased, leading to the spectrum of the almost complete alignment to the magnetic field. At 25°C, the axially symmetric powder pattern appeared again. This spectrum changed to a broad envelope of the powder pattern with round edges at 20°C due to the presence of a large amplitude motion in addition to a rotational motion about the molecular axis by lateral diffusion of the lipid molecule. The presence of a large amplitude motion is further revealed by the results that the chemical shift anisotropy, $\Delta\delta = \delta_{//} - \delta_{\perp}$, is decreased as the temperature is lowered from 25° to 20°C (Table 1). At 10°C, the isotropic ^{31}P NMR signal is dominated near 0 ppm because of the isotropic rapid tumbling motion of small particles caused by melittin-induced lysis of larger vesicles. The same axially symmetric powder patterns appeared again when the temperature was raised from 10° to 25°C as a result of fusion to form larger spherical vesicles. At a temperature above 30°C, the single perpendicular component appeared at −12 ppm, arising from the anisotropic ^{31}P chemical shift tensor of liquid crystalline bilayers (38). This result indicates that the lipid bilayer surface is oriented parallel to the magnetic field with a higher order of alignment by forming longer elongated vesicles (Fig. 5) referred to the MOVS (29).

Morphological changes of DLPC and DPPC bilayers containing melittin by ^{31}P NMR

Temperature variations of the ^{31}P NMR spectra of the DLPC and DPPC bilayers containing melittin, respectively, were observed to clarify the dependence of the lipid chain lengths on the respective morphological changes. The axially symmetric powder pattern was observed for the melittin-DLPC bilayers at 30°C, whereas the perpendicular component alone was observed from the melittin-DPPC bilayers at 50°C. The parallel edge became rounded when the temperature was lowered to 10°C and 40°C for the melittin-DLPC and -DPPC bilayers, respectively. The intensities of the perpendicular peaks were significantly decreased at 0°C and 35°C to result in the round powder patterns over the entire spectra for the melittin-DLPC ($Tc = 0$°C for the neat DLPC) and -DPPC ($Tc = 42$°C for the neat DPPC) (39) bilayers, respectively. This pattern alteration is attributable to increased additional motion beside the axially symmetric rotational motion of the lipid molecules. The anisotropies of these patterns differ substantially from those of gel phase with the ^{31}P chemical shift anisotropy of ~60 ppm in saturated lecithin bilayers (38). Besides, the chemical shift

TABLE 1 Temperature variations of ^{31}P chemical shift anisotropies of phospholipids in melittin-lecithin bilayer systems

	DLPC ($Tc = 0$°C)*				DMPC ($Tc = 23$°C)*				DPPC ($Tc = 42$°C)*			
	30°C	10°C	0°C	−10°C†	40°C	25°C	20°C	10°C†	50°C	40°C	35°C	20°C†
$\delta_{\perp}$/ppm	−10.1 ± 0.2	−10.2 ± 0.4	−8.6 ± 0.6	−0.9 ± 0.3	−12.3 ± 0.2	−12.7 ± 0.4	−9.6 ± 0.8	−1.3 ± 0.4	−11.1 ± 0.2	−11.1 ± 0.2	−10.3 ± 0.4	−0.8 ± 0.3
$\delta_{//}$/ppm	18.5 ± 0.3	19.4 ± 0.5	17.5 ± 0.8	−0.9 ± 0.3	20.1 ± 0.3	18.4 ± 0.6	16.6 ± 1.2	−1.3 ± 0.4	n.d.‡	21.4 ± 0.4	17.7 ± 0.6	−0.8 ± 0.3
$\Delta\delta$/ppm§	28.6	29.6	26.1	0	32.6	31.1	26.2	0	n.d.‡	32.5	28.0	0

*Van Dijck et al. (39).
†Only isotropic signals were observed from the lipids.
‡Not detected.
§$\Delta\delta = \delta_{//} - \delta_{\perp}$.

anisotropies were decreased near the respective *T*cs (Table 1), proving that the reduced anisotropy was caused by an additional large-amplitude motion of lipid molecules.

When the temperature was lowered to −10°C and 20°C for the melittin-DLPC and -DPPC bilayers, respectively, isotropic peaks due to small membrane fragments appeared at −0.9 and −0.8 ppm, respectively. The broadened isotropic components for the melittin-DLPC bilayers at −10°C can be attributable to a lowered fluidity of the solvent. The perpendicular component remarkably increased as the temperature was raised to 10°C and 40°C for the melittin-DLPC and -DPPC, respectively. When the temperature was further raised to 30°C and 50°C for the melittin-DLPC and -DPPC bilayers, respectively, only the sharp perpendicular component alone was observed at −10.1 and −11.1 ppm, respectively, by forming long elongated vesicles.

These findings based on the static ^{31}P NMR spectra indicate that the melittin-DLPC, -DMPC, and -DPPC bilayers are spontaneously aligned to the magnetic field, with the membrane plane being parallel to the magnetic field by forming elongated vesicles at a temperature above the *T*c. It is also found that significant morphological changes for the three melittin-lecithin bilayers occur accompanied by a large amplitude motion of lipid molecules near the respective *T*c.

Potassium ion leakage from lipid bilayer vesicles

It has been reported for the melittin-DMPC bilayers that small unilameller vesicles were formed when the temperature was raised above the *T*c and the discoidal bilayers were formed below the *T*c (6). On the other hand, these results of microscopic observations indicate that multilameller giant vesicles were formed at a temperature above the *T*c in the case where 9 mol % of melittin molecules were incorporated in the DMPC bilayers. Therefore, we have further examined whether the vesicles and/or pores are formed in the bilayers above or below the *T*c, as viewed from the leakage of entrapped potassium ions within the bilayer vesicles by using a potassium ion selective electrode. Fig. 6 shows the manner of potassium ion leakage by adding Triton X-100 solution into the lipid dispersed solution to dissolve the lipid bilayers in the buffer. It was clearly observed that the potassium ions were retained in the vesicles and leaked immediately after adding Triton X-100 solution at a temperature above the *T*c (40°C). In contrast, the potassium ions were not leaked at a temperature below the *T*c (2°C). These results clearly indicate that bilayer vesicles were not formed below the *T*c and hence the potassium ions were not trapped. It is also noticed that large vesicles were formed at a temperature above the *T*c and they entirely burst, because the potassium ion leakage was observed only after a first drop of Triton X-100 solution. This result also indicates that even small pores were not formed far above the *T*c since the trapped potassium ions did not leak at 40°C.

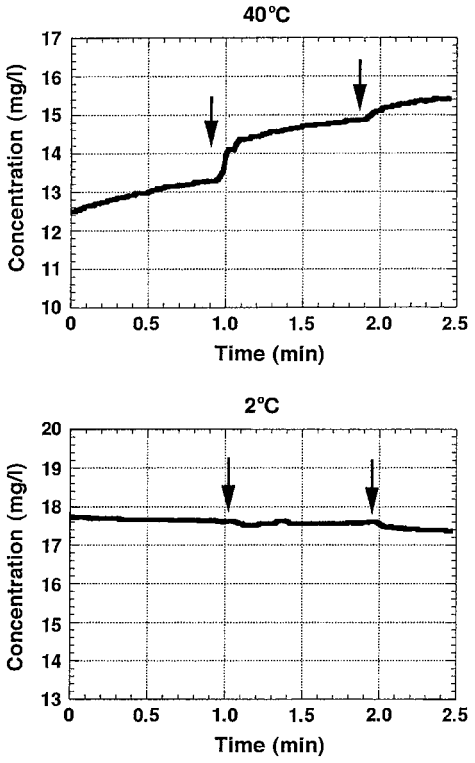

FIGURE 6 Plots of potassium concentration measured by a potassium ion-selective electrode as a function of time at 40°C (*top*) and 5°C (*bottom*), respectively, in the presence of melittin-DMPC lipid bilayer dispersions. 1 ml of 5% m/v Triton-X solution was added at the time of the arrow positions.

Molecular association disclosed from MALDI-TOF MS spectrometry

Fig. 7 shows the MALDI-TOF MS spectra of melittin after the reaction with the linker molecules (Fig. 7 *A*) in the DMPC bilayers at various temperatures. A monomer peak of melittin appeared at the mass number of 2849 accompanied by the peaks at 3003 and 3158, corresponding to the melittin molecules linked with one and two linker molecules (Fig. 7 *B*), respectively. Interestingly, a dimer peak with the mass number of 5839 was not significant at 35°C (above the *T*c), but the intensity of the peaks greatly increased at 25°C (near the *T*c) and 15°C (below the *T*c). This finding indicates that melittin molecules are connected by the linker molecules in the lipid bilayers and form dimers at a temperature near and below the *T*c, because the melittin molecules are closely located to each other at these temperatures. Namely, melittin can associate with each other to exhibit phase separation at 25°C (*right insets* of Fig. 7 *B*) as indicated in a fluorescent microscope. This molecular association allows linkage of neighbor melittin molecules with the linker molecule. Below the *T*c (15°C), the disc type particles are formed and the edge parts are surrounded by the melittin molecules so that again the melittin molecules can locate in the vicinity of the other

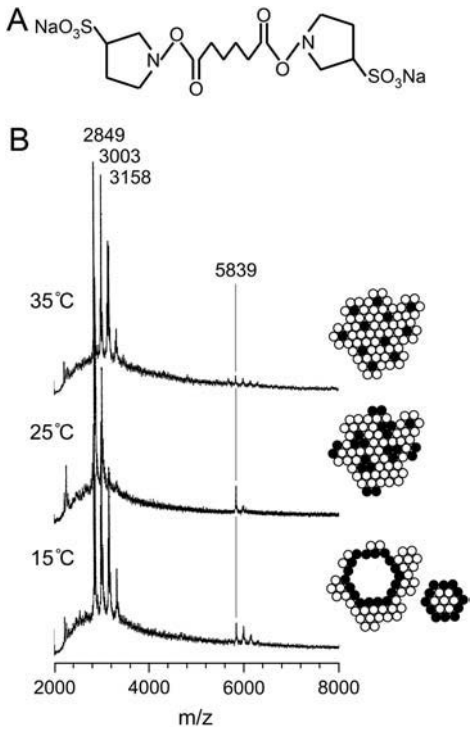

FIGURE 7 MALDI-TOF MS spectra of melittin after the reaction with the linker molecules in the DMPC bilayers. (*A*) Structure of linker molecule, BS^2. (*B*) Temperature variation of the MALDI-TOF MS spectra of the melittin-DMPC bilayer systems. The peaks with the mass number of 5839 correspond to the melittin dimer connected by the linker molecule. The solid and open circles indicate melittin and lipid molecules, respectively.

melittin molecules and dimers can form connected by the linker molecules. In contrast, melittin exists mainly as a monomer or antiparallel dimer surrounded by lipids at 35°C because linker molecules cannot make dimers in those states of melittin molecules.

DISCUSSION

Property of magnetic alignment of melittin-lecithin bilayer

In this study, we found that partially magnetic alignment was established for the bilayers hydrated by Tris buffer, immediately after the sample was inserted in the magnetic field at a temperature above the *T*c. It was also confirmed that after taking the sample below the *T*c, a very good alignment to the magnetic field was established after raising the temperature above the *T*c. Since the lecithin constitutes giant vesicles with the diameters of ~20 μm as demonstrated in our previous report (28), the elongated vesicle can be formed along the applied magnetic field as a result of gaining the total orientation energy (40). This energy due to a negative anisotropy of the magnetic susceptibility of lipid molecules (41) is accumulated as a result of reconstitution of the elongated giant vesicles through fusion of membrane fragments in the presence of the magnetic field. The elongated vesicles are thus capable of magnetic alignment exceeding the energy of a thermal fluctuation as the temperature is raised above *T*c.

On the other hand, it is evident from the ^{31}P NMR spectra that melittin causes the greatest perturbation to the bilayer structure near the *T*c. Such fluctuation of the lipids not only causes a melittin-mediated membrane fusion (vesiculation) and membrane disruption (solubilization) but also breaks down the magnetic alignment. This is because a large amplitude motion of the lipid molecules (a fluctuation of lipid axis) causes reduction of the anisotropy of the magnetic susceptibility so that vesicles cannot have enough energy to align to the magnetic field. It is also noticed that the viscosity of the melittin-DMPC bilayer dispersion was increased when the temperature was increased to that above the *T*c. This indicates that lipid bilayer vesicles cooperatively interact each other to orient to the magnetic field at a temperature above the *T*c.

Molecular mechanism of fusion and lysis in the melittin-lecithin bilayer systems

It is of interest to discuss the molecular mechanism of fusion and lysis in the melittin-lecithin bilayer systems. In this microscopic observation, it is evident that melittin is strongly bound to the vesicles and distributed homogeneously at a temperature above the *T*c. When a temperature is close to the *T*c, melittin molecules associate with each other to cause phase separation as observed in fluorescent microscopy. Consequently, a large amplitude fluctuation of lipid molecules occurs near the *T*c, as shown in the microscopic picture of Fig. 1 *B* and illustrated in Fig. 8. In our previous study, we showed that melittin forms the pseudotransmembrane

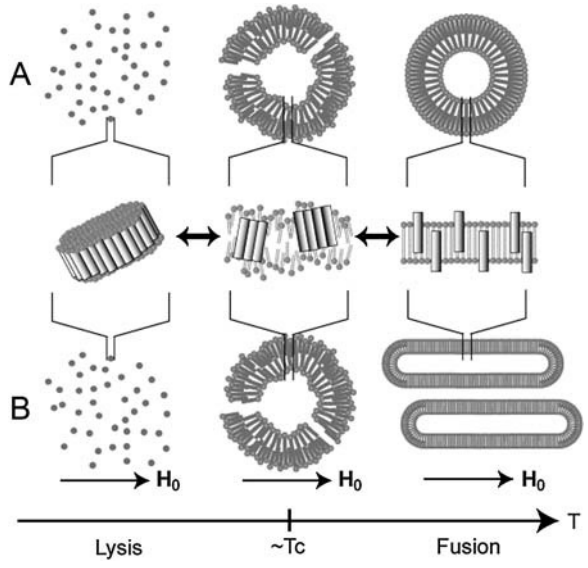

FIGURE 8 Schematic representation on the process of morphological changes in the melittin-lecithin bilayer systems in the absence (*A*) and presence (*B*) of applied magnetic field.

α-helix with an amphiphilic nature (28,29). Nevertheless, melittin can stay homogeneous as antiparallel helix dimers or monomers that dynamically form bundles in the hydrophobic environments when the lipid bilayer takes liquid crystalline phase above the *T*c. At a temperature close to the *T*c, a large number of melittin molecules associate with each other by facing the hydrophilic side together and facing the hydrophobic side to the lipids to cause a larger phase separation (*right insets* of Fig. 7 *B*) and partial disorder of lipids (Fig. 8). This associated melittin was further observed as a dimeric form with the linker molecules as judged from MALDI-TOF MS measurements.

When a temperature is below the *T*c, bundles of melittin molecules associate with each other. Consequently, small lipid bilayer particles are surrounded by the belt of melittin to be released from the vesicle to cause a large size of pores and consequently bring about the membrane disruption. This large size of pores may be similar to barrel-stave type pores rather than toroidal pores proposed for magainin (42,43). Subsequently, entire vesicles are dissolved into the buffer solution. On the other hand, when a temperature is slightly above the *T*c, a small number of associated melittin molecules causes a large amplitude motion of lipids in addition to the motion about the molecular axis as shown in Fig. 8. This large amplitude motion of lipids may cause the surface of vesicles to fluctuate, causing the mixing of lipids between the two vesicles and consequently vesicle fusion.

CONCLUSIONS

Giant vesicles with the diameters of $\sim$20 μm as a result of fusion were clearly seen in the melittin-lecithin bilayers with the molar ratio of 1:10 above the *T*c in various melittin-lecithin systems. Fusion and lysis of the vesicles were clearly visible by microscopic measurements above and below the *T*c, respectively. It turned out that the vesicles became blurred at a temperature slightly above the *T*c and a dynamic pore formation was seen at the temperature. Subsequently, complete fragmentation occurs at a temperature below the *T*c for the lecithin bilayers containing melittin. This fusion and lytic behavior around the *T*c can be explained by the fact that melittin molecules taking the pseudotransmembrane α-helices associate with each other to cause phase separation. As a result, induced large amplitude motion of lipids causes the membrane fusion of vesicles above the *T*c. On the other hand, a large number of associated melittin molecules cause fragmentation of vesicles below the *T*c.

SUPPLEMENTARY MATERIAL

An online supplement to this article can be found by visiting BJ Online at http://www.biophysj.org.

The authors thank Professor T. Shimmen and Dr. S. Sonobe of Himeji Institute of Technology for their advice on measuring the microscope.

This work was supported, in part, by Grants-in-Aid for Scientific Research from the Ministry of Education, Culture, Sports, Science and Technology of Japan.

REFERENCES

1. Habermann, E., and J. Jentsch. 1967. Sequenzanalyse des melittins aus den tryptischen und peptischen spaltstücken. *Hoppe Seylers Z. Physiol. Chem.* 348:37–50.
2. Sessa, G., J. H. Freer, G. Colacicco, and G. Weissmann. 1969. Interaction of a lytic polypeptide, melittin, with lipid membrane systems. *J. Biol. Chem.* 244:3575–3582.
3. Tosteson, M. T., and D. C. Tosteson. 1981. Melittin forms channels in lipid bilayers. *Biophys. J.* 36:109–116.
4. Kempf, C., R. D. Klausner, J. N. Weinstein, J. Van Renswoude, M. Pincus, and R. Blumenthal. 1982. Voltage-dependent trans-bilayer orientation of melittn. *J. Biol. Chem.* 257:2469–2476.
5. Habermann, E. 1972. Bee and wasp venoms. *Science*. 177:314–322.
6. Dufourc, E. J., J. F. Faucon, G. Fourche, J. Dufourcq, T. Gulik-Krzywicki, and M. le Maire. 1986. Reversible disc-to-vesicle transition of melittin-DPPC complexes triggered by the phospholipids acyl chain melting. *FEBS Lett.* 201:205–209.
7. Dufourc, E. J., I. C. P. Smith, and J. Dufourcq. 1986. Molecular details of melittin-induced lysis of phospholipid membranes as revealed by deuterium and phosphorus NMR. *Biochemistry*. 25: 6448–6455.
8. Dempsey, C. E. 1990. The actions of melittin on membranes. *Biochim. Biophys. Acta*. 1031:143–161.
9. Dufourcq, J., J. F. Faucon, G. Fourche, J. L. Dasseux, M. Le Maire, and T. Gulik-Krzywicki. 1986. Morphological changes of phosphatidylcholine bilayers induced by melittin: vesicularization, fusion, discoidal particles. *Biochim. Biophys. Acta*. 859:33–48.
10. Dempsey, C. E., and B. Sternberg. 1991. Reversible disc-micellization of dimyristoylphosphatidylcholine bilayers induced by melittin and [Ala-14]melittin. *Biochim. Biophys. Acta*. 1061:175–184.
11. Dempsey, C. E., and A. Watts. 1987. A deuterium and phosphorous-31 nuclear magnetic resonance study of the interaction of melittin with dimyristoylphosphatidylcholine bilayers and the effects of contaminating phospholipase A2. *Biochemistry*. 26:5803–5811.
12. Monette, M., and M. Lafleur. 1995. Modulation of melittin-induced lysis by surface charge density of membranes. *Biophys. J.* 68:187–195.
13. Beschiaschvili, G., and J. Seelig. 1990. Melittin binding to mixed phosphatidylglycerol/phosphatidylcholine membranes. *Biochemistry*. 29:52–58.
14. Talbot, J. C., J. Dufourcq, J. de Bony, J. F. Faucon, and C. Lussan. 1979. Conformational change and self association of monomeric melittin. *FEBS Lett.* 102:191–193.
15. Lauterwein, J., L. R. Brown, and K. Wüthrich. 1980. High-resolution ^{1}H-NMR studies of monomeric melittin in aqueous solution. *Biochim. Biophys. Acta*. 622:219–230.
16. Bazzo, R., M. J. Tappin, A. Pastore, T. S. Harvey, J. A. Carver, and I. D. Campbell. 1988. The structure of melittin. A ^{1}H-NMR study in methanol. *Eur. J. Biochem.* 173:139–146.
17. Brown, L. R., J. Lauterwein, and K. Wüthrich. 1980. High-resolution ^{1}H-NMR studies of self-aggregation of melittin in aqueous solution. *Biochim. Biophys. Acta*. 622:231–244.
18. Terwilliger, T. C., and D. Eisenberg. 1982. The structure of melittin. *J. Biol. Chem.* 257:6010–6015.
19. Terwilliger, T. C., L. Weissman, and D. Eisenberg. 1982. The structure of melittin in the form I crystals and its implication for melittin's lytic and surface activities. *Biophys. J.* 37:353–361.
20. Inagaki, F., I. Shimada, K. Kawaguchi, M. Hirano, I. Terasawa, T. Ikura, and N. Go. 1989. Structure of melittin bound to perdeuterated

dodecylphosphocholine micelles as studied by two-dimensional NMR and distance geometry calculations. *Biochemistry.* 28:5985–5991.

21. Okada, A., K. Wakamatsu, T. Miyazawa, and T. Higashijima. 1994. Vesicle-bound conformation of melittin: transferred nuclear Overhauser enhancement analysis in the presence of perdeuterated phosphatidylcholine vesicles. *Biochemistry.* 33:9438–9446.
22. Citra, M. J., and P. H. Axelsen. 1996. Determination of molecular order in supported lipid membrane by internal reflection Fourier transform infrared spectroscopy. *Biophys. J.* 71:1796–1805.
23. Altenbach, C., W. Froncisz, J. S. Hyde, and W. L. Hubbell. 1989. Conformation of spin-labeled melittin at membrane surfaces investigated by pulse saturation recovery and continuous wave power saturation electron paramagnetic resonance. *Biophys. J.* 56:1183–1191.
24. Stanislawski, B., and H. Rüterjans. 1987. ^{13}C-NMR investigation of the insertion of the bee venom melittin into lecithin vesicles. *Eur. Biophys. J.* 15:1–12.
25. Dempsey, C. E., and G. S. Butler. 1992. Helical structure and orientation of melittin in dispersed phospholipid membranes from amide exchange analysis in situ. *Biochemistry.* 31:11973–11977.
26. Hristova, K., C. E. Dempsey, and S. H. White. 2001. Structure, location, and lipid perturbation of melittin at the membrane interface. *Biophys. J.* 80:801–811.
27. Smith, R., F. Separaovic, T. J. Milne, A. Whittaker, F. M. Bennett, B. A. Cornell, and A. Makriyannis. 1994. Structure and orientation of the pore-forming peptide, melittin, in lipid bilayers. *J. Mol. Biol.* 241:456–466.
28. Naito, A., T. Nagao, K. Norisada, T. Mizuno, S. Tuzi, and H. Saitô. 2000. Conformation and dynamics of melittin bound to magnetically oriented lipid bilayers by solid-state ^{31}P and ^{13}C NMR spectroscopy. *Biophys. J.* 78:2405–2417.
29. Toraya, S., K. Nishimura, and A. Naito. 2004. Dynamic structure of vesicle-bound melittin in a variety of lipid chain lengths by solid-state NMR. *Biophys. J.* 87:3323–3335.
30. Lam, Y.-H., S. R. Wassall, C. J. Morton, R. Smith, and F. Separovic. 2001. Solid-state NMR structure determination of melittin in a lipid environment. *Biophys. J.* 81:2752–2761.
31. Frey, S., and L. K. Tamm. 1991. Orientation of melittin in phospholipids bilayers. A polarized attenuated total reflection infrared study. *Biophys. J.* 60:922–930.
32. Pott, T., and E. J. Dufourc. 1995. Action of melittin on the DPPC-cholesterol lipid-ordered phase: a solid state ^{2}H- and ^{31}P-NMR study. *Biophys. J.* 68:965–977.
33. Scholz, F., E. Boroske, and W. Helfrich. 1984. Magnetic anisotropy of lecithin membranes: a new anisotropy susceptometer. *Biophys. J.* 45:589–592.
34. Seelig, J., F. Borle, and T. A. Cross. 1985. Magnetic ordering of phospholipids membranes. *Biochim. Biophys. Acta.* 814:195–198.
35. Speyer, J. B., P. K. Sripada, S. K. Das Gupta, G. G. Shipley, and R. G. Griffin. 1987. Magnetic orientation of sphingomyelin-lecithin bilayers. *Biophys. J.* 51:687–691.
36. Brumm, T., A. Möps, C. Dolainsky, S. Brückner, and T. M. Bayerl. 1992. Macroscopic orientation effects in broadline NMR-spectra of model membranes at high magnetic field strength: a method preventing such effects. *Biophys. J.* 61:1018–1024.
37. Qiu, X., P. A. Mirau, and C. Pidgeon. 1993. Magnetically induced orientation of phosphatidylcholine membranes. *Biochim. Biophys. Acta.* 1147:59–72.
38. Smith, I. C. P., and I. H. Ekiel. 1984. Phosphorus-31 NMR of phospholipids in membranes. *In* Phosphorous-31 NMR: Principles and Applications. D. G. Gorenstein, editor. Academic Press, Orlando, FL. 447–475.
39. Van Dijck, P. W. M., B. de Kruijff, L. L. M. Van Deenen, J. de Gier, and R. A. Demel. 1976. The preference of cholesterol for phosphatidylcholine in mixed phosphatidylcholine-phosphatidylethanolamine bilayers. *Biochim. Biophys. Acta.* 455:576–587.
40. Naito, A., T. Nagao, M. Obata, Y. Shindo, M. Okamoto, S. Yokoyama, S. Tuzi, and H. Saitô. 2002. Dynorphin induced magnetic ordering in lipid bilayers as studied by ^{31}P NMR spectroscopy. *Biochim. Biophys. Acta.* 1558:34–44.
41. Boroske, E., and W. Helfrich. 1978. Magnetic anisotropy of egg lecithin membranes. *Biophys. J.* 24:863–868.
42. Matsuzaki, K., O. Murase, N. Fujii, and K. Miyajima. 1996. An antimicrobial peptide, magainin 2, induced rapid flip-flop of phospholipids coupled with pore formation and peptide translocation. *Biochemistry.* 35:11361–11368.
43. Yang, L., T. A. Harroun, T. M. Weiss, L. Ding, and H. W. Huang. 2001. Barrel-stave model or toroidal model? A case study on melittin pores. *Biophys. J.* 81:1475–1485.